CHISA'96

12th International Congress
of Chemical and Process Engineering
25–30 August 1996, Praha, Czech Republic
Scientific Committee

Mail: Congress CHISA, P. O. Box 857, 111 21 Praha 1 Fax: +42 2 342073 E-mail: chisa@icpf.cas.cz

23 July, 1996

L. M. Uliev
Kharkov State Polytech. Univ.
ul. Frunze 21
310002 Kharkov
Ukraine

Dear Participant,

I would like to apologize for the bug which appeared in our database program. Due to this we have reported wrong date of your presentation. The correct information is provided below.

I am pleased to inform you that your paper has been included in the Final Program of the Congress as follows:

Paper No.: E2.4 Ref. No.: 0272
Authors: Tovazshnyanski, L. L., Kapustenko, P. A., Uliev, L. M., *Perevertilenko, A. Yu. (asterisk denotes the author delivering the paper)
Affiliation: State Polytech. Univ., Kharkov, Ukraine
Title: The design of optimum geometry of corrugated plates in plate heat exchangers

Presentation: lecture, Monday 15.45 Duration: 30 min

I am sorry for inconvenience which was caused to you.

I am looking forward to meeting you in Prague.

Sincerely yours,

Ivan Wichterle
Scientific Committee

THE DESIGN OF OPTIMUM GEOMETRY OF CORRUGATED PLATES IN PLATE HEAT EXCHANGERS

L.L. Tovazhnyanski, P.A. Kapustenko, L.M. Uliev, A.Yu. Perevertilenko
Kharkov State Polytech. Univ., Dep. Chem. Eng., Frunze St. 21, 310002, Kharkov, Ukraine;
Tel. (380) 572-400-893, Fax. (380) 572-400-632, E-mail: ulm@lotus.kpi.kharkov.ua

The mastering of new resource saving technology is the important problem which determines the increase of national income in the industry. For the branch of heat transfer equipment this problem can be solved by reduction of the overall dimensions and specific metal capacity of the heat exchangers. This paper deals with the solution of the named problem with designing of the plate heat exchangers which are the most perspective equipment in this branch [1].

Because experimental selection of optimum geometry of the heat exchanger surface is very expensive the interest to the creation of scientifically based research and calculation methods for elements of heat exchange equipment is growing now.

Modelling of convection heat transfer in channel with corrugated walls (Figure 1) is very complicated, through intricate three-dimensional flow of fluid. The solution of differential equation of transfer for turbulence flow, which is more interesting practically, is not always possible even for rectilinear channels [2]. So the pressure drop with fluid flow for constant properties in the plate heat exchanger may be calculated with the help of Darcy's law [3].

$$\Delta P = \xi \frac{L}{d_e} \frac{\rho V^2}{2} . \tag{1}$$

The expression for calculation ξ we found with the help of statistic treatment of the experimental data received for the channels which are distinguished from one another by the geometry of corrugations [4]:

$$\xi = \frac{0.34 \exp(1.51\,\mathrm{tg}\varphi)}{\mathrm{Re}^{0.25-0.06\,\mathrm{tg}\varphi}} \left[1.24 \exp(-0.37\,\mathrm{tg}\varphi)\right]^{\beta}, \tag{2}$$

where β– parameter geometry size of corrugation, what depends on its height -h and distance between adjacent crests- l.

The width of the entry and exit section corresponded width of the channel, i.e., redistribution of the base of liquid flow was not there.

Using of (2) by the method of modified thermal hydrodynamics analogy the expression for the heat transfer coefficient was obtained, too [5]:

$$\alpha = \frac{0.14\,\lambda\,\mathrm{Re}\,\mathrm{Pr}\sqrt{\xi}}{d_e\left\{\ln\left(\mathrm{Re}\frac{\sqrt{\xi}}{760}\right) + 2\frac{\mathrm{Pr} + \ln(1+5\mathrm{Pr})}{\sqrt{\vartheta}}\right\}}, \tag{3}$$

where ϑ- the function of pressure gradient.

The dependence (1) is correct for flow in the porous medium, too [6], because of to cell structure of channel the flow between corrugated plates we can consider as two-dimensional flow in porous medium between smooth parallel plates, i.e., as non linear analogue of the cell Hele-Shaw in shape of the plate heat exchanger [7,8].

The relationship (1) we can write in form

$$\frac{dP}{dL} = -kf(V), \tag{4}$$

where k dependent only from geometric parameters of the channel, f(v) – as a rule, is power function of velocity [3]. For two-dimensional flow we can express the pressure gradient as:

$$\frac{dP}{dx_i} = -k_{ij} f_j(\vec{V}), \tag{5}$$

were k_{ij} – tensor value which characterise the resistance of medium to flow and it is on its physical sense inverse to the tensor of penetrability in the theory of filtration, V – the filtration velocity of liquid.

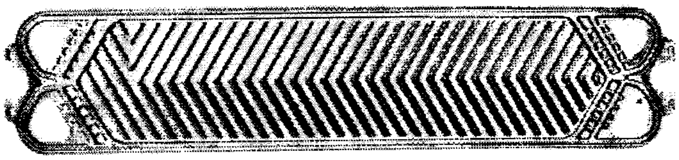

Figure 1. The plates of heat exchanger of the type 0.3 E.

The medium of interplate channel can be considered as orthtropic because the corrugation of plates and their position (Figure 1) allow to choice two mutually orthogonal directions on which the values of coefficients of resistance are extreme. In the system of co-ordinates connected with the main axises of tensor k_{ij} (Figure 2) the gradient of pressure is written down in canonical form as:

$$\mathrm{grad}P = -\vec{i}k_x \mathrm{sign}(V_x)|V_x|^{s_x} - \vec{j}k_e \mathrm{sign}(V_y)|V_y|^{s_y}, \tag{6}$$

where s_x, s_y= s(β, x, y); κ_x ,κ_y - the coefficients of resistance along and across of the channel.

We introduce the dimensionless variables and parameters

$$\Pi = \frac{(P-P_0)d_e^2\rho}{\mu^2},\ Rv_x = \frac{d_e V_x \rho}{\mu},\ Rv_y = \frac{d_e V_y \rho}{\mu},\ \Lambda = \frac{d_e}{L},\ \chi = \frac{x}{L},\ \eta = \frac{y}{L}, \tag{7}$$

and write projection of equation (5) on co-ordinate axises and continuity equation in the form

$$\Lambda \frac{\partial \Pi}{\partial \chi} = -\kappa_x \mathrm{sign}(Rv_x)|Rv_x|^{s_x}, \tag{8}$$

$$\Lambda \frac{\partial \Pi}{\partial \eta} = -\kappa_y \mathrm{sign}(Rv_y)|Rv_y|^{s_y}, \tag{9}$$

$$\frac{\partial Rv_x}{\partial \chi} + \frac{\partial Rv_y}{\partial \eta} = 0. \tag{10}$$

The boundary conditions for this set of equations will be conditions of impenetrable on the sides and constant gradients of pressure on entry in the channel and on exit from it, given by constant flowrate of fluid (Figure 2)

$$\left(\frac{1}{\kappa_x}\frac{\partial \Pi}{\partial \chi}\right)^{2/s_y} + \left(\frac{1}{\kappa_y}\frac{\partial \Pi}{\partial \eta}\right)^{2/s_y} = Re_o^2, \qquad \begin{cases} 0 \le \eta \le \eta_1; \\ \eta_2 \le \eta \le \eta_0; \end{cases} \quad 0 \le \chi \le \frac{\chi_0}{2}, \tag{11}$$

$$\left(\frac{1}{\kappa_x}\frac{\partial \Pi}{\partial \chi}\right)^{2/s_y} + \left(\frac{1}{\kappa_y}\frac{\partial \Pi}{\partial \eta}\right)^{2/s_y} = 0, \qquad \begin{cases} 0 \le \eta \le \eta_1; \\ \eta_2 \le \eta \le \eta_0; \end{cases} \quad \frac{\chi_0}{2} \le \chi \le \chi_0, \tag{12}$$

$$\frac{\partial \Pi}{\partial \chi} = 0,\quad \eta_1 \le \eta \le \eta_2, \qquad \begin{cases} \chi = 0; \\ \chi = \chi_0, \end{cases} \tag{13}$$

where $\eta_1 = y_1/L$; $\eta_2 = y_2/L$; $\eta_0 = 1$; $\chi_0 = H/L$.

These conditions were written for "left" of the channel, for "right" they were written similar.

Let us differentiate the equation (8) and (9) with respect to corresponding co-ordinate. Then we can get derivatives of velocities, substituting which in continuity equation we get up the expression describing the field of pressure in the channel of plate heat exchanger:

$$\kappa_y s_y Rv_y^{s_y-1}\frac{\partial^2\Pi}{\partial\chi^2}+\kappa_x s_x Rv_x^{s_x-1}\frac{\partial^2\Pi}{\partial\eta^2}=0, \tag{14}$$

$$Rv_x=-\mathrm{sign}\left(\frac{\partial\Pi}{\partial\chi}\right)\kappa_x^{-1/s_x}\left(\Lambda\left|\frac{\partial\Pi}{\partial\chi}\right|\right)^{1/s_x}, \tag{15}$$

$$Rv_y=-\mathrm{sign}\left(\frac{\partial\Pi}{\partial\chi}\right)\kappa_y^{-1/s_y}\left(\Lambda\left|\frac{\partial\Pi}{\partial\chi}\right|\right)^{1/s_y}. \tag{16}$$

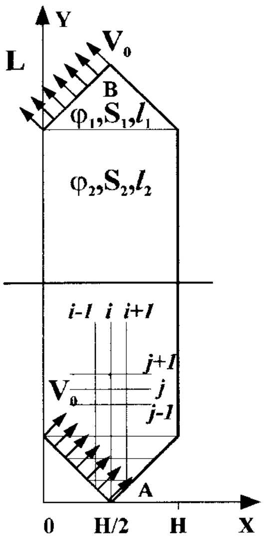

Figure 2. Scheme of the channel and numerical grid.

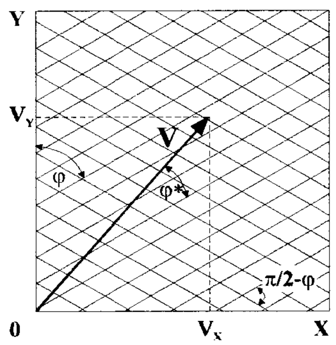

Figure 3. To the definition of the angle between filtration velocity and corrugation.

The set of equations (11)-(16) were integrated numerically by the method of transition to a steady state. For this the equation (12) was written in non-stationary form, i.e. the left part of it was equalled to derivative $\partial\Pi/\partial\tau$, where τ is some dimensionless time. Space derivations were approximated by centre finite differences on numerical grid (Figure 2). The set of ordinary differential equations describing the pressure Π_{ij} in each grid-point was obtained. These equations were integrated by method of Gear [9] to reach the steady state. The constant of flowrate was check for each cross-section on the grid during calculation.

Integration of obtained set gives the distributions of dimensionless pressure and components of velocity on the field of heat transfer area.

With the help of this data and expression (3) we should obtain the distribution of heat transfer coefficient on plate, but previously it is need to define for any direction of filtration velocity in the channel between plates (Figure 3).

The expression (2) was obtained with condition that V was directed along the plate and φ was the angle of inclination of corrugation to direction of velocity. The angle of corrugation's inclination to stream change on $\pi/2$-φ with the changing of velocity direction on $\pi/2$ (Figure 3). This allows to define an angle of corrugation's inclination to stream φ^* if components V_x and V_y are know, i.e.ξ in equation (3) will be defined for the angle:

$$\varphi^*=\varphi+\left(1-\frac{4\varphi}{\pi}\right)\left|\mathrm{arctg}\left(\frac{V_x}{V_y}\right)\right|. \tag{17}$$

The distribution of velocity in adjacent channels is symmetric about main axis of the plate with equal conditions for heat-transfer medium, i.e. the heat transfer coefficients will be symmetric, too:

$$\left|V'_{i,j}\right| = \left|V''_{N+1-i,j}\right| \rightarrow \alpha'_{i,j} = \alpha''_{N+1-i,j}, \tag{18}$$

where '-for left channel, "-for right, i=1,2,.....,N, j=1,2,......M. The overall heat transfer coefficients, in this case, are defined as:

$$K_{i,j} = \left(\frac{1}{\alpha_{i,j}} + \frac{\delta_p}{\lambda_p} + \frac{1}{\alpha_{N+1-i,j}}\right)^{-1}, \tag{19}$$

where $\delta_p = 10^{-3}$ m, $\lambda_p = 60$ W $m^{-1}K^{-1}$, -the thickness and thermal conductivity of the plate.

This model shows significant divergence between calculation results and experimental results, obtained on the standard heat exchangers with the plates of type 0,6 [3,10]; where $\varphi = 60°$ on whole field of the plate, L= 1,1 m, H= 0,55 m, l= 18 mm, h = 4 mm. The experiments were performed for liquid with parameters: c= 4,174 kJ/kg·K, μ= 0,4997·10^{-3} Pa·s, λ_e= 0,648 W·m^{-1}·k^{-1}. Comparison shows that average errors for calculation of pressure drop and mean overall heat transfer coefficient are somach 15% (Figure 4).

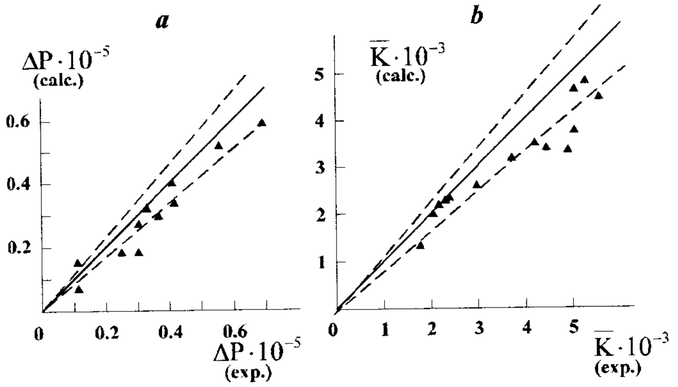

Figure 4. Comparison of the calculated values of pressure drop (a) and average overall heat transfer coefficient (b) with experimental results (points); the solid lines- that is ideal coincidence, the dashed lines - boundaries of 15% deviations. ΔP, Pa, K -W $m^{-2}k^{-1}$.

Similar investigations were performed for widely used low heat exchangers with plates of type P 0,6-2 [10], which have on allocation section the angle of corrugation inclination to main axis of plate 15° and on base field $\varphi = 40°$ (Figure 2). In this case the condition of conjugation must be performed for a section with different angles φ:

$$\frac{1}{\kappa_{y1}\Delta\eta_1}\left(\frac{\partial\Pi}{\partial\eta}\right)_1 = \frac{1}{\kappa_{y2}\Delta\eta_2}\left(\frac{\partial\Pi}{\partial\eta}\right)_2, \tag{20}$$

where $\Delta\eta_1$, $\Delta\eta_2$- the length of steps on grid in the η- direction for section 1 and 2 (Figure 2).

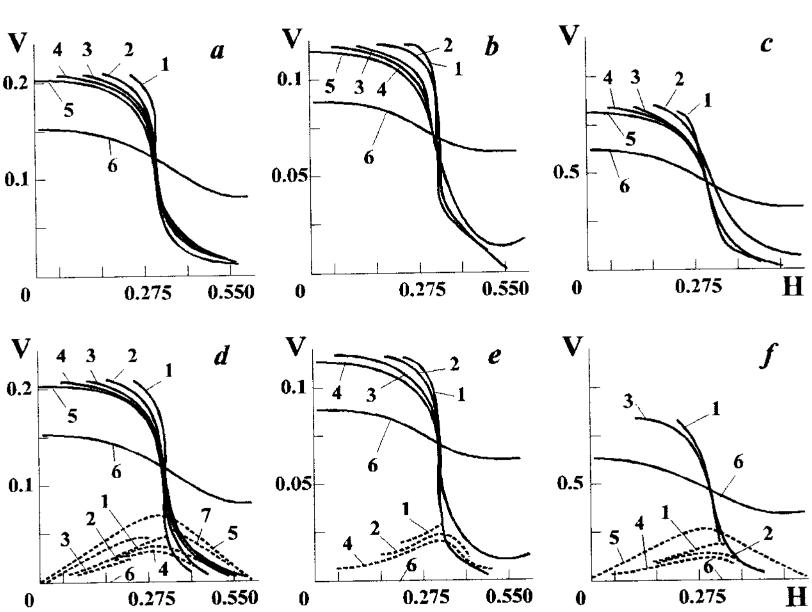

Figure 5. The distributions of velocity modulus (a, b, c) and components V_x (solid line), V_y (dashed line) (d, e, f) for heat exchanger of type P 0.6-2 across of the channel; a, d -Q= 0,278 10^{-3} m^3c^{-1}; b, e - 0,956 10^{-3}; the distance from beginning of the plate: 1-4 sm, 2-8, 3-12, 5- 20, 6- 55, 7- 28 sm. V, m s^{-1}; H, m.

In this case the resistance to flow along the plate is significantly less than across the

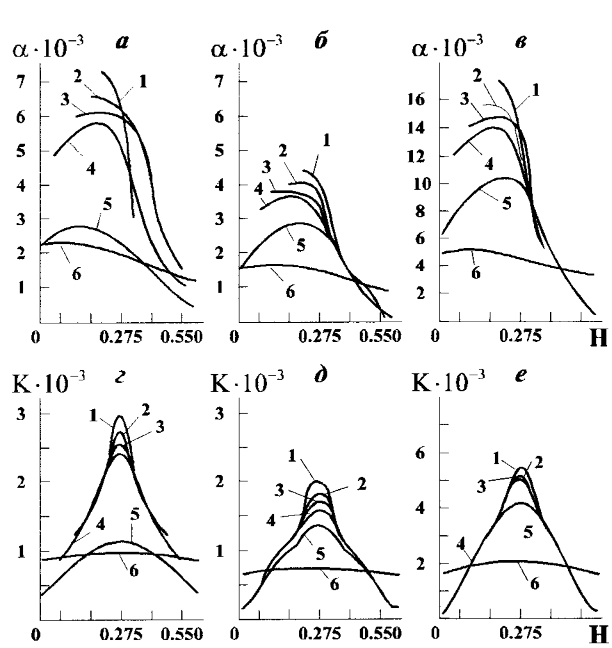

Figure 6. The distributions of the heat exchanger coefficient α overall heat exchanger coefficient K across of the channel. Designation is alike to figure 5. α, W·m^{-2}K.

plate ($\kappa_{x1}/\kappa_{y1} \approx 80$, $\kappa_{x2}/\kappa_{y2} \approx 6$) in consequence of that the liquid has not time uniformly to distribute on cross-section of the channel and the velocity of liquid on collector side is the biggest for any cross-section (Figure 5). Owning to such distribution of the velocity the distribution of heat transfer coefficient is very uniformly on the cross of plate (Figure 6), and this leads to the stretched in shape of a pike distributions of overall heat transfer coefficient across the plate.

On the distribution section of plate the modulus of velocity is slightly bigger than on base field because the cross-section here is less. Here the value V_x is bigger, so the distribution of the fluid stream across the channel occur here. Then V_x decreases to 0 and the flow becomes practically rectilinear (Figure 5). Owing to such distribution of velocity the heat transfer and overall heat transfer coefficient on entry sections are higher than on the base field (Figure 7). However the distribution of K is symmetric to main axis of the plate owing to symmetry of α distribution in the adjacent channels. The presented results show that in heat exchangers P 0,6-2 the corrugations of the plates are njt proper designed, at the least on the entry and exit sections.

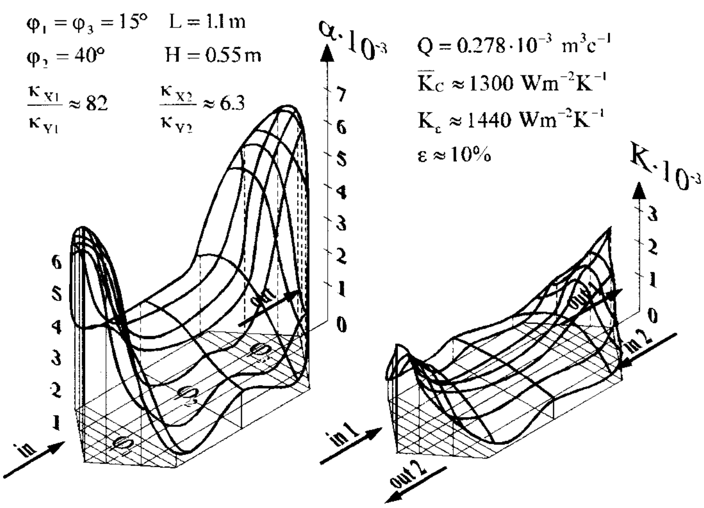

Figure 7. The distribution of coefficients α and K for the plate P0.6-2 ($\overline{K_c}$-calculate value, $\overline{K_e}$-experimental).

The influence of the changes in corrugated field of plates on heat exchange was investigated by numerically for the plates of type 0,6 and their modifications.

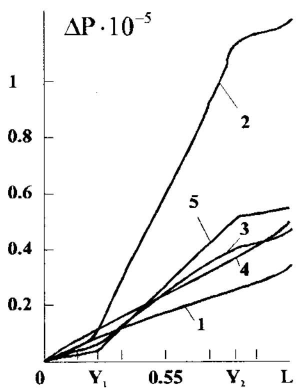

Figure 8. The pressure drop distribution along the channel: 1- for variant a)-2 for b), 3- for c), 4- for d). L, m.

Let us consider the heat exchanger with flow rates in adjacent channels Q=0,137·10^{-2}m^{3}c^{-1} for five variants of corrugated field:

a) $\varphi_1 = \varphi_2 = 60°$, $l_1 = l_2 = 18$ mm, $h_1 = h_2 = 4$ mm;

b) $\varphi_1 = 60°$, $\varphi_2 = 60°$, $l_1 = l_2 = 18$ mm, $h_1 = h_2 = 4$ mm;

c) $\varphi_1 = 70°$, $\varphi_2 = 65°$, $l_1 = 36$ mm, $l_2 = 18$ mm, $h_1 = h_2 = 4$ mm;

d) $\varphi_1 = \varphi_2 = 60°$, $l_1 = l_2 = 18$ mm, $h_1 = h_2 = 3$ mm;
e) $\varphi_1 = 70°$, $\varphi_2 = 65°$, $l_1 = 36$ mm, $l_2 = 18$ mm, $h_1 = h_2 = 3$ mm.

The distribution of pressure along the channel is defined by shape of plate corrugation. In the cases a) and d) it is almost linear as corrugation of the plates is uniform.

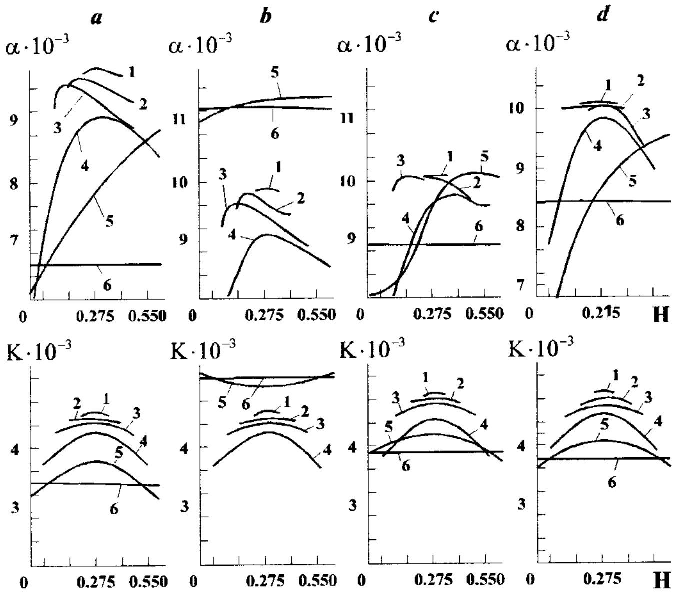

Figure 9. The distribution of heat exchanger and overall heat exchange coefficients across the channel for variants a), b), c) and d) (a-d accordingly); the distance on axis y from beginning of the plate is: 1- 4 sm, 2- 8, 3- 12, 4- 16, 5- 24, 6- 55 sm.

In other cases the angle of corrugation inclination on the boundaries of distribution sections changes abruptly because the resistance to flow and grad P change too (Figure 8). The heat transfer coefficient has similar distribution on the plate field.

Where value grad P is big they reach the maximum values (Figure 9). With it on the distribution regions

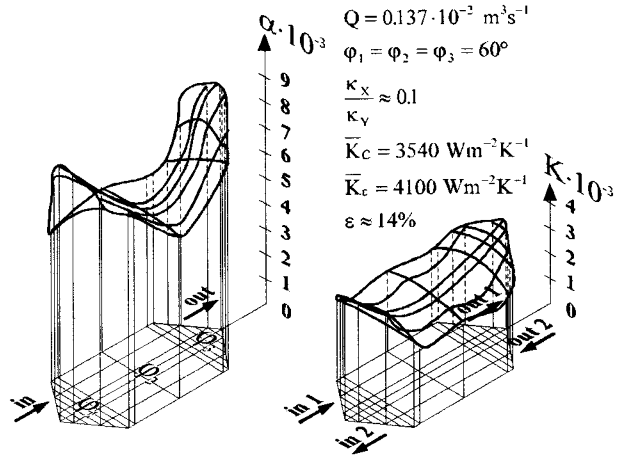

Figure 10. The distributions of the coefficients α and K on the field of plate for variant a).

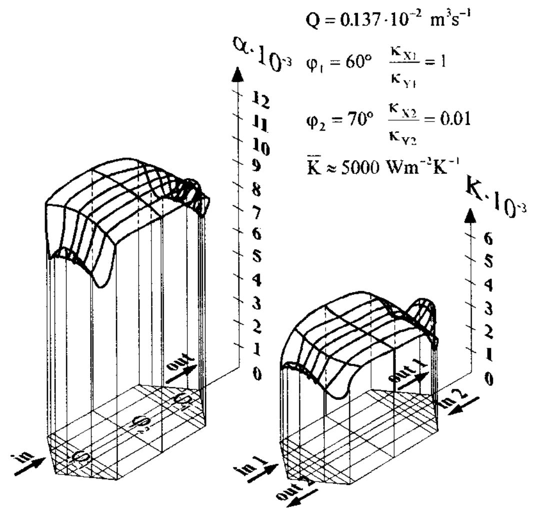

Figure 11. The distributions of the coefficients α and K on the field of plate for variant b).

the profile α is not symmetric so that here the profile of velocity is not formed yet. For variants a) and d) it is more expressed (Figure 9,10). In case b) $\kappa_{y2} > \kappa_{y1}$, and $\kappa_{y1}/\kappa_{x1} \approx 0{,}1$, $\kappa_{y2}/\kappa_{x2} \approx 0{,}01$ that promotes more uniform distribution of liquid on cross-section of the channel. Therefore α

Figure 12. The experimental plate with "S" corrugations.

and K on the entry and exit are distributed more uniformly and on the base field of plate their values are higher than on the distribution regions (Figure 11). The average overall heat transfer coefficient $\overline{K}$ for variant b) is higher on 41.2% than in initial variants a). But ΔP, however, increases on 243%. In the case c) $\overline{K}$ increases on 24,3% in comparison with a) and ΔP on 40%. In the cases d) and e) the increasing of $\overline{K}$ is less than average comparative mistake and ΔP increases significantly and we can say that the change of corrugated field is more favorably for variant c).

The plate with curvilinear "S" - alike corrugations (Figure 12) was designed for treat-

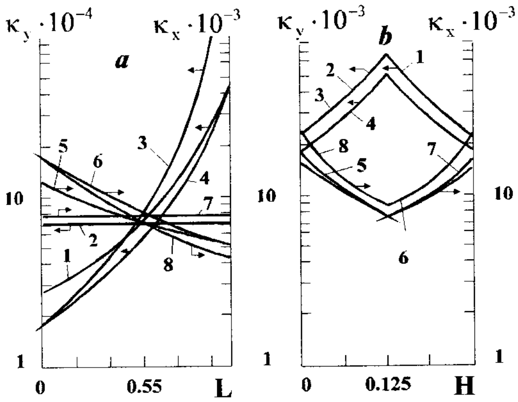

Figure 13. The distributions of resistance coefficients: a) along of center axis of channel, b-across of the channel for y= L/2; 1, 2, 3, 4-distribution of κ_y; 5, 6, 7, 8-κ_x; 1, 5- for "S" corrugation with the change of inclination along the center line 50°-70°; 2, 7 "S" corrugation with inclination on axis 60°; 3, 8 - 45°-75°; 4, 6 - 45°-70°, L, m.

ment of high-viscosity liquids [11-13]. The numerical and physical experiments were performed to define the efficiency of these plates with treatment of liquid with constant properties. The investigation were done on base of the plate 0.3 E with L=1.1, H=0,25 m, h= 4 mm, R = 0.7; the distance between next crests along center axis l_0 = 20 mm with the following variants of corrugations: 1) the plate of type herringbone pattern with φ = 60°; 2) the plate with "S"-alike corrugations and with constant angle of their inclination along the center axis φ = 60°; 3) "S"-alike corrugations with the change of inclination angle along the center axis from 45° to 70°; 4) "S"-corrugations with the change φ_0 from 45° to 70°; 5) "S"-corrugations with the change φ_0 from 50° to 70°. The properties of fluid kept previous and flow rate is $Q = 5 \cdot 10^{-4}\ m^3c^{-1}$. The distribution κ_x and κ_y for the chosen cases are shown on the figure 13.

As in the channels with "S" -alike corrugation of plates κ_x and κ_y are functions of coordinates so the equation (12) must be recast as:

$$\kappa_y s_y Rv_y^{s_y-1}\left(\Lambda \frac{\partial^2 \Pi}{\partial \chi^2} + Rv_x^{s_x}\frac{\partial \kappa_x}{\partial \chi}\right) + \kappa_x s_x Rv_x^{s_x-1}\left(\Lambda \frac{\partial^2 \Pi}{\partial \eta^2} + Rv_y^{s_y}\frac{\partial \kappa_y}{\partial \eta}\right) = 0, \qquad (21)$$

where it is taken into account that the coefficients κ depend on φ stronger than power s.

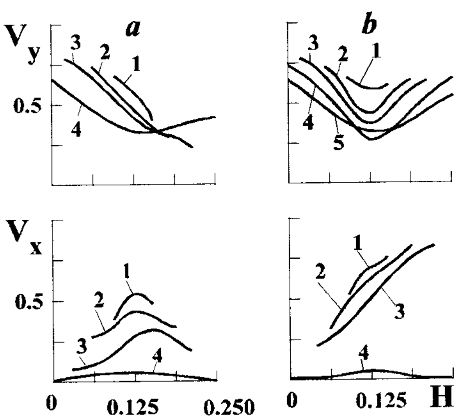

Figure 14. The distributions of the velocity components across the channel: a - for the plate of the type herringbone pattern, b- for the plate with "S" corrugations where φ_0=60°; 1-y= 0.025m, 2-0.05, 3-0.075, 4-0.1, 5-0.19, 6-0.55m.

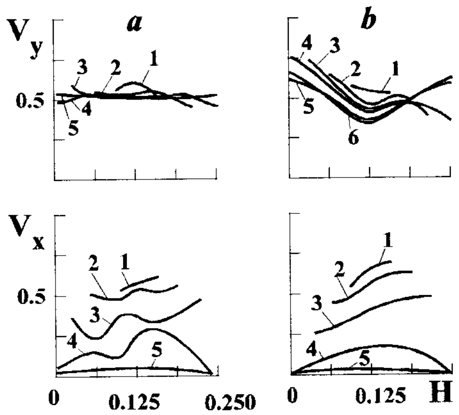

Figure 15. The distribution of the velocity components across the channel for the plate with "S" corrugations and changing their inclination along center line 45°-70°; a - first half of the plate; 1-y= 0.025m, 2-0.05, 3-0.075, 4-0.1m; b) - second half; 1-L-y= 0.025m; 2-0.05, 3-0.075, 4-0.1, 5-0.55m.

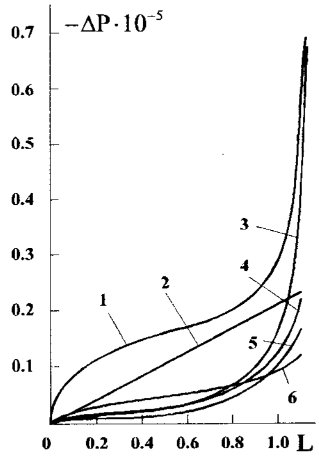

The boundary conditions the method of solution remain previous.

In case 1) the resistance to flow along the channel is slightly more than across the channel, and the length of the channel is significantly bigger than its width that favours to set up the uniform profile of velocity (Figure 14).

Figure 16. The pressure drop distribution along the center line of channel; 1- for plate with "S" corrugation and φ=70°-75°, 2- "fir", 3-φ=45°-75°, 4-50°-70°, 5-45°-70°.

In the channels with plates of case 2) the distributions κ_x and κ_y in cross-section are non-uniformly: κ_y is maximum in the center and it decreases to periphery of the channel, and conduct of κ_x is reverse. This means that resistance to liquid motion along the channel on periphery will be less and the stream of fluid there will be more than in center (Figure 14).

In accordance with such distribution of stream on the distribution region the cross component of velocity V_x is rather higher for 2 case than for 1 and the biggest part of the fluid directs to periphery of the channel.

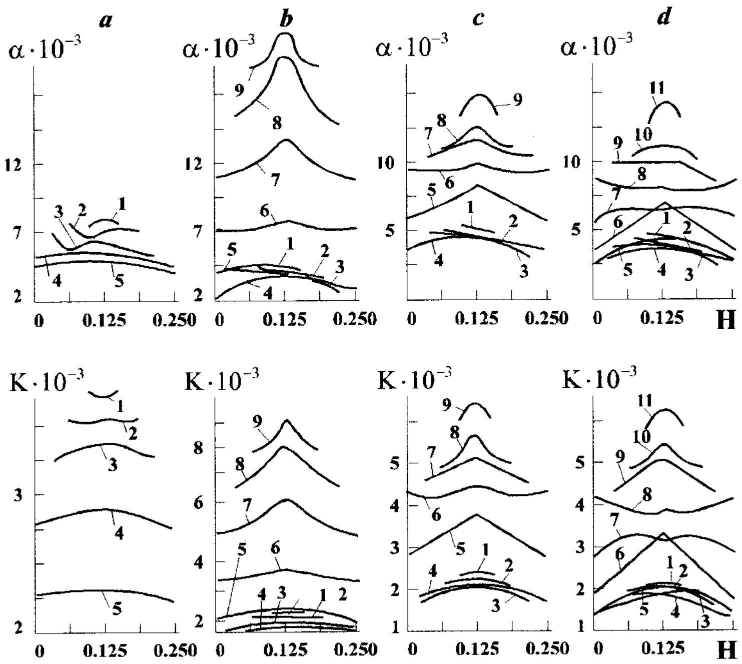

Figure 17. The distributions of α and K across the channel: a-for variant 1) 1-y= 0.025 m, 2-0.05, 3-0.075, 4-0.1, 5-0.55m; b, c- for variants 4) and 5); 1-y=0.025 m, 2-0.05, 3-0.075, 4-0.1, 5-0.19, 6-0.55, 7-1.025, 8-1.05, 9-1.075 m, d) - for variant 3) 1-y=0.025 m, 2-0.05, 3-0.075, 4-0.1, 5-0.19, 6-0.55, 7-0.31, 8-0.81, 9-1.025, 10-1.05, 11-1.075, 11-1.075m.

If in the cases 1) and 2) the distribution of velocities is symmetric about the center of plate line then for cases 3) and 4) there is no such symmetry. On the entry where angle inclination of corrugation is small, $\kappa_x >> \kappa_y$ because the liquid has not time to distribute uniformly on width of entry region, and owing to this V_y in within the distribution region is higher at the collector hole (Figure 15). Further the distribution of liquid velocity is analogously to distribution in 2) case as the resistance to motion of liquid on periphery is less than in the center. However on the exit because of $\kappa_y >> \kappa_x$ (the inclination of corrugation is big) the cross component of velocity increases (Figure 15). The distribution of pressure is determined, in the main, by the character of resistance coefficients of distribution. The distribution of pressure is almost linear for uniform of their distribution (Figure 16). In case 2) the gradient of pressure is less than in case 1) as the resistance to flow on periphery of the channel is less. For variants 3), 4), and 5) ΔP is significant less than in first two cases as the inclination of corrugation to axis here is less, i.e. and κ_y is less. But then along the channel the inclination of corrugation to axis increases, that leads to sharp increasing of pressure drop on the exit from the channel where region of flow almost is partitioned off by corrugations with the inclination near to 75°.

The distributions of heat transfer coefficients are alike to distribution of pressure gradient. In the case 1) α has maximum on the distribution regions where absolute value of velocity is maximum (figure 17). In the cases 3)- 5) the heat transfer coefficient firstly decreases on entry because of diminishing of velocity modulus but then with increasing φ_0 it increases. The distribution of overall heat transfer coefficients is alike to distribution of α (Figure 18). For case 1) when the distributions κ_x and κ_y are uniform we obtain sufficiently even distribution α and K. In the cases 3)- 5) in the beginning of flow where the inclination of corrugation is not significance yet, the distributions α and K are almost uniformly (Figure 17), although the velocity is increased to periphery of the channel, but κ_y is decreased to periphery that leads to even distribution of heat transfer coefficient. With further flow K is increased in accordance with α (Figure 19).

Table I. The comparison of pressure drop ΔP and average overall heat transfer coefficient K for different types of plates.

No.	Type of plate	$\Delta P \cdot 10^{-5}$, Pa	Deviation ΔP from No. 1, %	K, $Wm^{-2}k^{-1}$	Deviation K from No. 1, %
1	herringbone pattern	0.23	0	2500	0
	«S»-corrugation				
2	φ_0=60°	0.124	-46	2960	18
3	φ_0=45-70°	0.96	-15	2900	16
4	φ_0=45-75°	0.615	167	3460	36
5	φ_0=50-70°	0.221	-4	3250	30

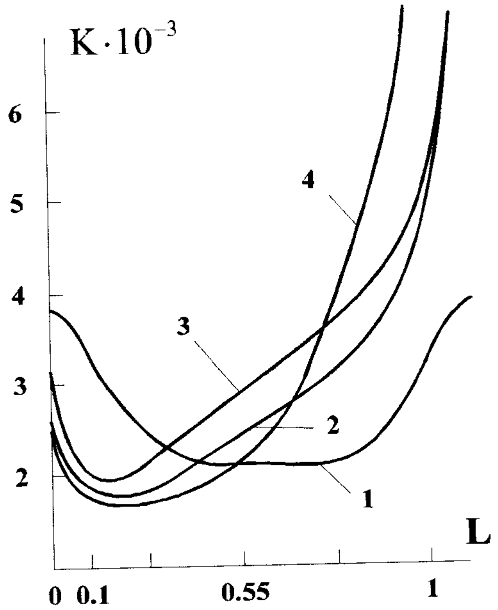

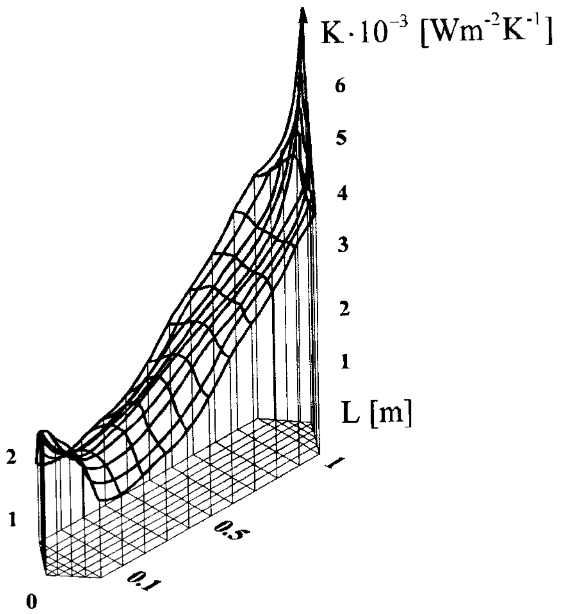

Figure 18. The distribution of overall heat transfer coefficient along the center axis of the plate: 1-for plate of the type herringbone pattern; 2- for plate with φ_0= 45°-70°; 3-for plate with φ_0= 50°-70°; 4- for plate with φ_0= 45°-75°.

Figure 19. The distribution of overall heat transfer coefficient on the field of plate with "S" corrugations and with the exchange of inclination along the center axis from 45° to 70°.

It is clear from table 1. that the plates with "S"-corrugations have greater K for lesser energy expenditures, except the fourth case where pressure drop is sharply increased on exit section because of big inclination of corrugations. Here we can make the conclusion that the plates with "S"-corrugations are more efficient. The experiments were performed for the text of the created model.

For this the flat sheet of the plate type 0.3 E was chosen and on it were brazed the wires alike to rectilinear and "S"-corrugations (Figure 12).

The comparison of heat flux obtained on a pressed plates with the flux obtained on the plates with the brazed rectilinear wires showed that pressed plates were more about 28% effective. The experiments performed on the plates shown on figure 12, allow to define that for equal of pressure drop the average overall heat transfer coefficient on the field of plate with "S"-corrugations is about 30% bigger than on the field of plate with brazed rectilinear wires.

NOMENCLATURES:

c-specific heat, J $kg^{-1}K^{-1}$; d_e-equivalent diameter, m; H- weight of plate, m; h- high of corrugation, m; M, N- numbers of steps in y and x directions; P, P_0 - pressure current and on entry, Pa; Q- flow rate, m^3s^{-1}; R- radius of curvature along "S" corrugation, m; x, y - Cartesian coordinates; $Re = Vde\rho/\mu$ -Reynolds number; $Re_0 = V_0 d_e \rho/\mu$ - Reynolds number on entry; $Pr = \mu c/\lambda_e$ Prandtl number; α-heat transfer coefficient, $Wm^{-2}K^{-1}$; δ-thickness of plate, m; λ-thermal conductivity, $Wm^{-1}K^{-1}$; φ-angle of corrugation inclination to center axis of plate, degree; φ_0 - angles of inclination on entry and exit, degree; μ- viscosity; Pa s; ρ- density, kg m^{-3}; κ- resistance coefficient.

Indices: x, y-directions along coordinates; p-plates, l-liquid; 1 - value for entry; 2- for base of field of plate.

REFERENCES

1. Butterwoth D., Mascone C.F. Heat transfer Heads into the 21st Century //CEP. 1991. Vol. 87. No. 9. P. 30-37.
2. Buleev N.I. Spatial model of turbulent exchange. - Moscow, Nauka, Main editorial board for Physical and mathematical literature, 1989. P. 344.
3. Kovalenko. L.M. Heat exchangers with intensification of heat exchange. M.1986.
4. Tovazhnyanski L.L., Kapustenko P.A., Cybulnik V.A. // Izv. Vuzov. Energetika. 1980. No. 9. P. 123-125.
5. Tovazhnyanski L.L., Kapustenko P.A. // Chem. Eng. Commun. 1984. Vol. 31. No. 6. P. 351-366.
6. Colliuz R.E. Flow of fluids through porous materials. Moscow. “Mir”. 1964.
7. Milne -Thomson L.M. Theoretical hydrodynamics. Moscow. "Mir". 1964. P.656.
8. Feder J. Fractals. - Moscow. "Mir". 1991. P.264.
9. Gear C.W. Numerical initial value problems in ordinary differential equation. Englewood Cliffs, N. J.: Prentice-Hall, 1971.
10. Plate heat exchangers. Catalog. M.,1983.
11. Inventor’s certificate No. 1778484 USSR. Pack of counter flow heat exchanger / Pertsev L.P., Gurov O.I., Lupir V.F., Kovalenko L.M., Derzhanova L.V., Uliev L.M., Drozdov V.V. Bulletin No. 44. 30.11.92.
12. Pertsev L.P., Uliev L.M., Potebnia G.F. // Thes. of Papers VIII Union conf. "Two - phase flow in energy machines and apparatuses". L., 1990. Vol. 1. P. 311-313.
13. Pertsev L.P., Uliev L.M., Potebnia G.F. // Thes. of Papers VIII Union conf. "Two - phase flow in energy machines and apparatuses". L., 1990. Vol. 3. P. 133-135.